Journal of Visualization, Vol. 5, No. 1 (2002) 95-103

Study on Variation of Thermal Image by Infrared Radiometer Influenced by Fluctuations of Environmental Factors

Kamoi, A. *[1] and Okamoto, Y. *[2]

*1 Grad. School of Science and Arts, University of East Asia, 2-1 Ichinomiya Gakuen-cho, Shimonoseki, Yamaguchi 751-8503, Japan.

*2 3-7-19 Higashioshima-cho, Hitachinaka, Ibaraki 235-5678, Japan.

Received 30 July 2001.
Revised 5 November 2001.

***Abstract*:** The infrared radiometer (IR) displays the radiation temperature distribution. Frequently, thermal images on a CRT display fluctuate and those radiation temperatures cannot be measured correctly. Therefore, we are frequently faced with the difficult problem of evaluating the detection limits on surface and internal flaws in construction and underground structures, and so on. Those difficulties are considered to be due to fluctuations of the meteorological and environmental factors, mainly influenced by solar radiation, wind velocity, atmospheric temperature, and so on. Our experimental study clarifies the relation between variations of the thermal images on the CRT of IR display and the environmental factors using an analysis of power spectral density.

***Keywords*:** thermal image, detection limit, environmental factors, fluctuation, power spectral density.

1. Introduction

Thermal image analysis obtained by IR thermographs has been widely applied to nondestructive tests in application fields like detecting flaws of construction structure, underground objects, and so on. It is reported that fluctuations of environmental factors have frequently created fluctuations of thermal image and also difficulty in its analysis (Okamoto et al., 1997). In a previous paper, the authors showed that fluctuations appeared in thermal images of soil surface were strongly influenced by the environmental factors such as irradiance, ambient temperature and wind velocity, which vary according to meteorological conditions (Kamoi and Okamoto, 2000). In this paper, the static and dynamic thermal images of soil surface with buried objects, concrete and plywood surfaces are measured and analyzed by spectral analysis.

2. Survey of Fluctuation Study

2.1 Concept of Fluctuation and Power Spectral Density

Fluctuations are observed in our living environment as a variety of thermo-physical phenomena. Those fluctuations appear as results of meteorological factors such as irradiance, atmospheric temperature, wind velocity, physical factors such as heat noise, brownian movement and human factors such as heart pulse, blood pressure, brain wave. Those fluctuations are variations with the lapse of time which appear as a noise in the vicinity of the mean value. They become significant, unless they are fluctuations of random noise. The complex Fourier component of variance on environmental factors $g(t)$ is expressed by Eq. (1).

$$F(f) = \int_{-\infty}^{\infty} g(t) e^{-i2\pi ft} dt \tag{1}$$

Fourier component $F(f)$ is the amplitude of wave with period T, $|F(f)|^2$and represents the energy. Then the power spectral density $P(f)$ expressed by PSD is defined by taking mean energy per unit time as expressed by Eq. (2) (Hino, 1998).

$$P(f) = \lim_{T \to \infty} \left[\frac{1}{T} |F(f)|^2 \right] \tag{2}$$

The white noise becomes constant independently of the frequency f if frequency and spectrum are expressed on the logarithmic axis, according to spectral analysis of fluctuation around the mean value. Therefore Eq. (2) gives power spectral density (PSD).

2.2 Review of Study on Power Spectral Density

The logarithmic value of PSD appearing in environment decreases inversely proportional to logarithm of f with slope from −1 to −2 corresponding to $1/f$ to $1/f^2$, respectively as shown in Fig. 1 (Musha, 1979). But it has been recognized that $1/f^2$ to $1/f^4$ spectrum corresponding to fluctuations of environmental factors were observed except the conventional $1/f$ spectrum. The systematic research on PSD relating to environmental factors and objects to be measured has been newly carried out by the authors (Kamoi and Okamoto, 2000a,b).

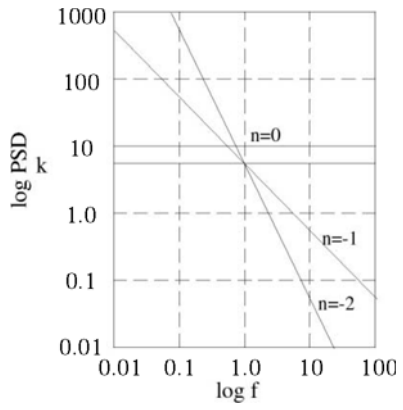

Fig. 1. PSD slope.

3. Experimental Apparatus

Figure 2 shows a schematic diagram of the experimental apparatus which consists of an infrared radiometer IR, model box (0.5 × 0.5 × 0.6 m) of the soil filled with heat insulation, digital recorder and sensors. The IR system consists of IR camera and control unit, and measures the radiation temperature distributions of soil, concrete and plywood surfaces by using IR camera with a Hg-Cd-Te sensor at 8-13 μm in the wavelength. In order to detect environmental factors there are pyranometer for irradiance (solar injection flux), anemometer for wind velocity and thermocouples with amplifier for detecting temperatures of atmosphere, soil, concrete and plywood surfaces.

4. Experimental Method

4.1 Concept of Fluctuation and Power Spectral Density

(1) Measurement of fluctuation: Environmental factors are irradiance, wind velocity, atmospheric temperature and humidity which give influence to the radiation temperatures on thermal images of soil, concrete and plywood surfaces. These values are stored in the digital recorder, as shown in Fig. 2. Each sensor has a time constant smaller than 1 s, and the sampling frequency of the digital recorder is 100 Hz. All temperatures are measured with an accuracy within ± 0.1 °C. In each fluctuation its value of RMS is calculated as STDEV by square root of variance of fluctuation.

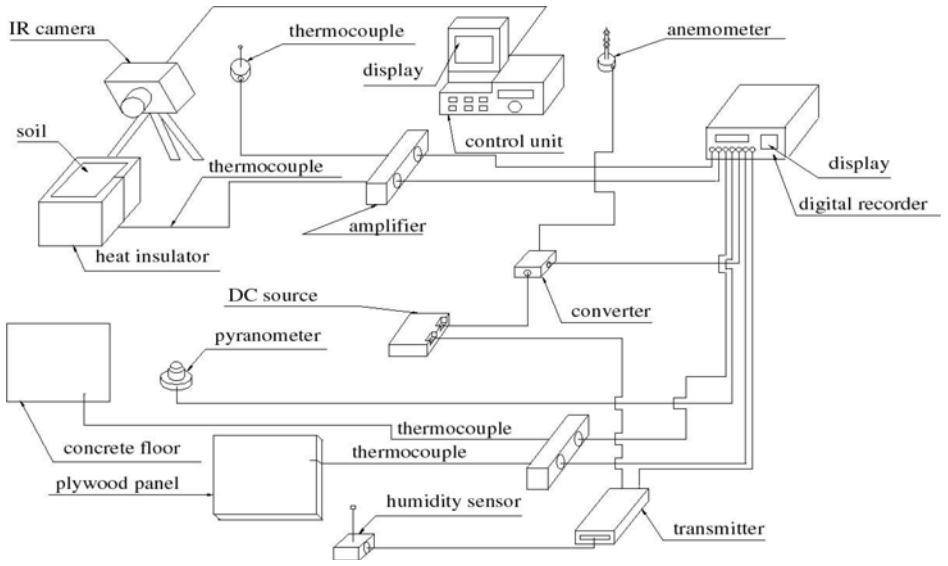

Fig. 2. Experimental apparatus.

(2) Measurement of thermal images: In order to investigate the variations appeared in the thermal images of soil surface, the static thermal images are measured outdoors and indoors by IR camera with an interval of 1 hr. The dynamic images are also measured after the static one at a specified point with frame time of 3 ms. The soil surface is settled parallel to the ground, and field of view is 0.4 rad. The thermal images are accordingly saved in the IR control unit.

4.2 Evaluation of Power Spectral Density (PSD)

PSD of the fluctuation data of four environmental factors and three objects which were saved in the digital recorder are calculated by the data analysis software called DADiSP. In the static thermal images of soil surface, PSD of the radiation temperature distributions along the center horizontal line are to be calculated. In its dynamic thermal images, PSD at the specified points on the center horizontal line during time tracing of 7.17 s are also calculated. In the graph of PSD each axis should be transformed to logarithmic one, with the respective scale being adjusted. Then, the profile of PSD becomes generally to be approximated by the lines with different decreasing slopes like Fig. 3. Therefore, each refracted line in the above graph is shown in Eq. (3).

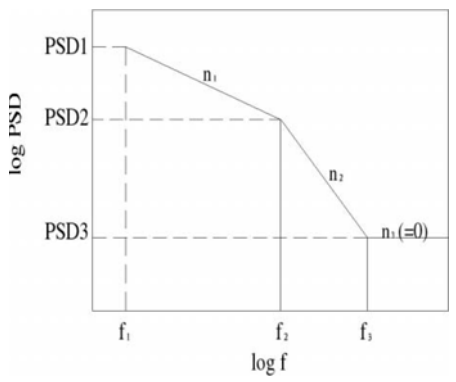

Fig. 3. Determination of slope n_1, n_2 (n_3=0) in the logarithmic graph.

$$\mathrm{PSD} = Kf^{n} \quad \log_{10}\mathrm{PSD} = \log_{10}K - n\log_{10}f \tag{3}$$

$$\log_{10}(\mathrm{PSD}_1 / \mathrm{PSD}_2) = \log_{10}(f_2{}^{n}/f_1{}^{n}) = \log_{10}(f_2/f_1)^{n}$$

$$n = \log_{10}(\mathrm{PSD}_1 / \mathrm{PSD}_2) / \log_{10}(f_2/f_1) \tag{4}$$

The above mentioned slope n is determined by Eq. (4) and also shown in Fig. 3.

5. Experimental Results and Consideration

5.1 Experimental Results

Figure 4 shows the variations of environmental factors versus time s like atmospheric temperature: $ta(t)$, humidity: $h(t)$, irradiance: $q(t)$ and wind velocity: $u(t)$ at 14:00 on November 28, 2000 (outdoors, cloudy). Fig. 5 also shows PSD characteristics versus frequency Hz by power spectral analysis of the variations of environmental factors as shown in Fig. 4.

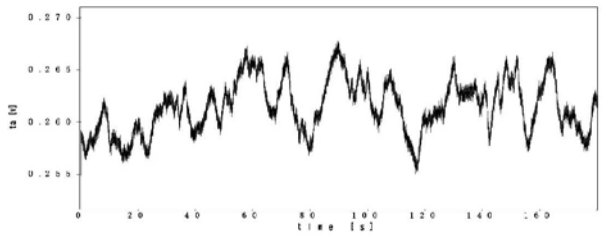

(a) *ta* (*t*) atmospheric temperature

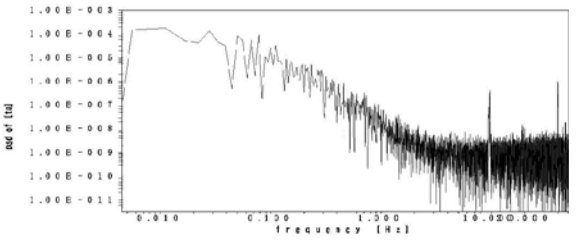

(a) *ta* (*t*) atmospheric temperature

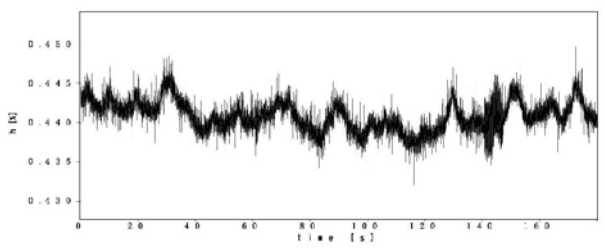

(b) *h* (*t*) atmospheric humidity

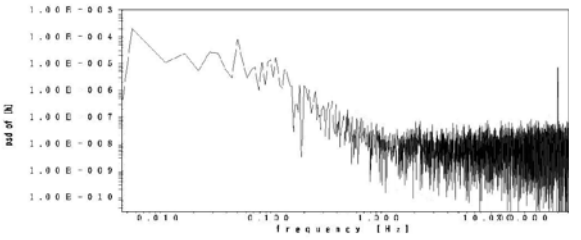

(b) *h* (*t*) atmospheric humidity

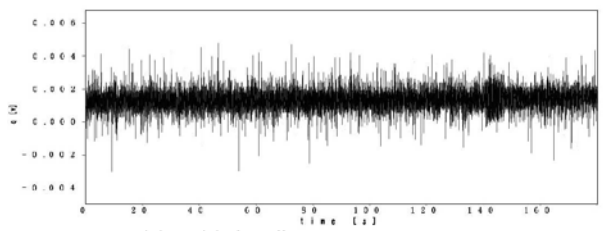

(c) *q* (*t*) irradiance

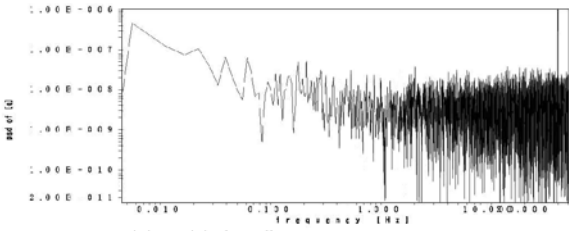

(c) *q* (*t*) irradiance

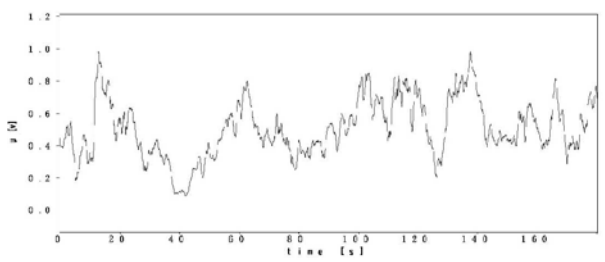

(d) *u* (*t*) wind velocity

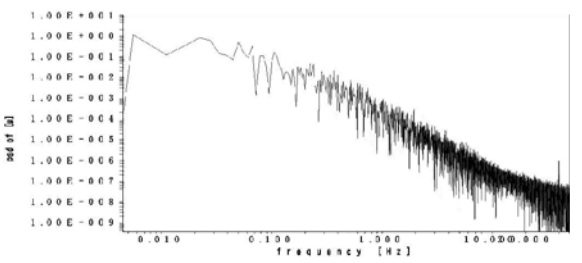

(d) *u* (*t*) wind velocity

Fig. 4. Variations of environmental factors.

Fig. 5. PSD characteristics of environmental factors.

Figure 6 is the static thermal images of soil surface at 16:00 and 19:00 on September 27, 2000 (outdoors, fair). In these thermograms the cross cursor line is shown, and there is a buried object (aluminum cylinder: ø 60 × 60 height mm) under the center of the cross cursor line. The radiation temperature distributions can be observed in bottom and left side of each thermal image corresponding to horizontal and vertical cursor line, respectively. Figure 7 shows PSD characteristics of the fluctuating radiation temperature on the horizontal cursor line of the static thermal images in Fig. 6.

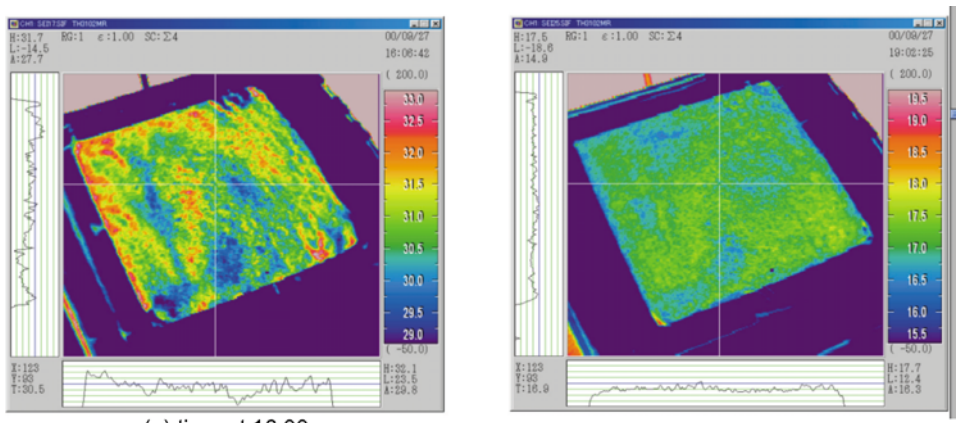

Fig. 6. Static thermal images.

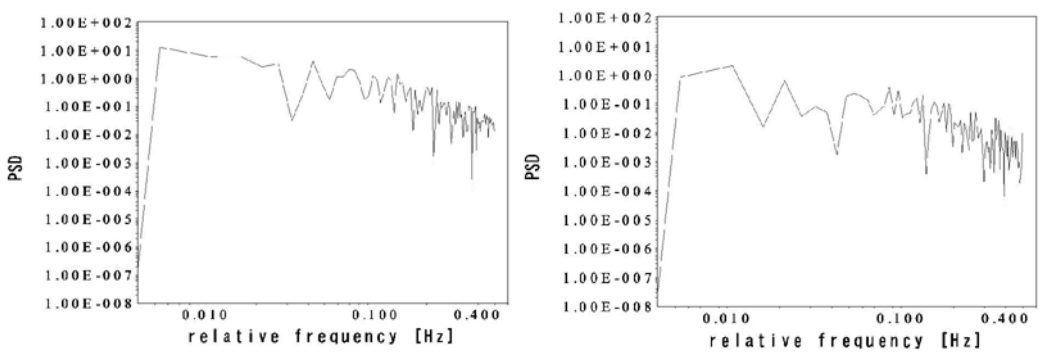

Fig. 7. PSD characteristics of static thermal images.

Figure 8 is the dynamic thermal images corresponding to the radiation temperatures of horizontal cursor lines on the static thermal images as shown in Fig. 6. The vertical multiple lines in the dynamic thermal image indicate time lapse. The variations of radiation temperatures were measured in the three points a, b and c on the above line. The point a corresponds to the location of the buried object. Figure 9 shows PSD characteristics of the fluctuating radiation temperature at the point a in Fig. 8.

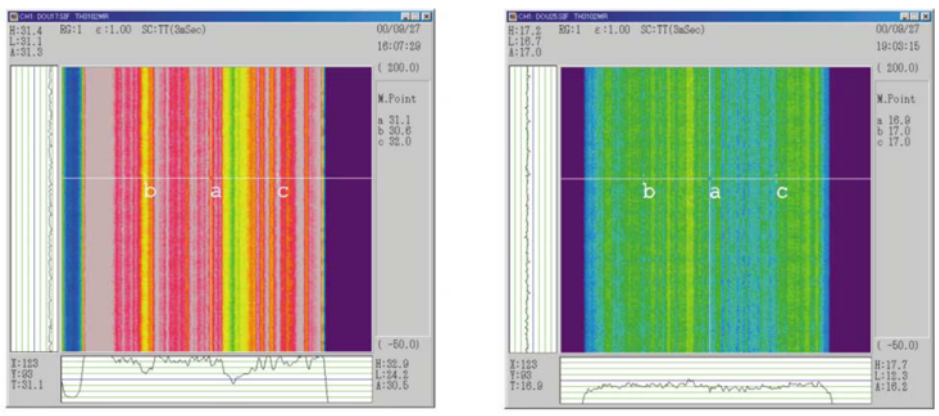

Fig. 8. Dynamic thermal images.

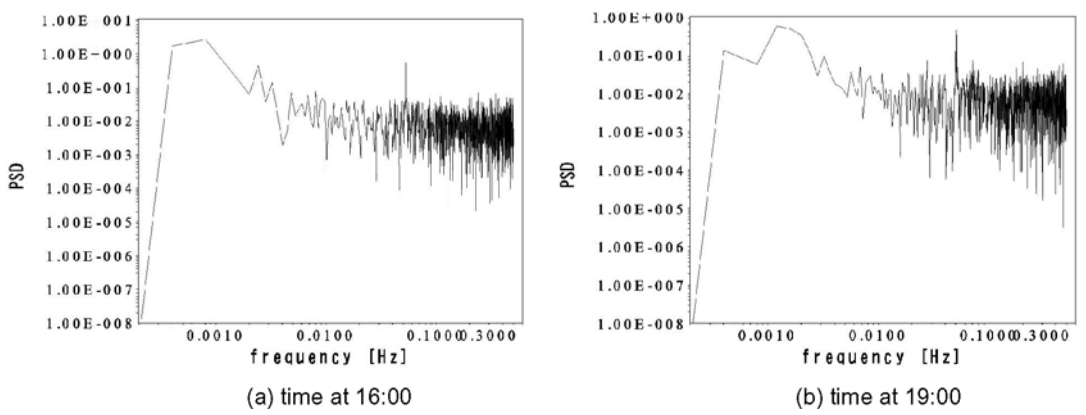

Fig. 9. PSD Characteristics of dynamic thermal images.

Figure 10 shows the fluctuating radiation temperature distribution on the horizontal cursor line in Fig. 6. Figure 11 shows the relation between PSD slope n_1 and RMS value versus time where expresses turbulence intensity in the static and dynamic thermal images for 11 hours on September 27, 2000. In Fig. 11, (a) is the case of horizontal cursor line in static thermal image and (b) is the case of point c in dynamic thermal image. Among many data in relation to environmental factors, objects and those thermal images were analyzed from June 2000 to January 2001.

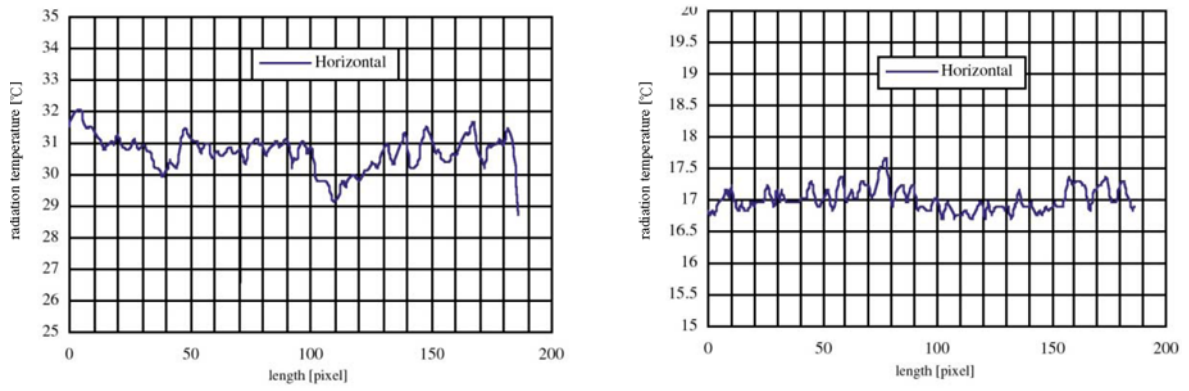

Fig. 10. Fluctuating radiation temperature distribution of static thermal images.

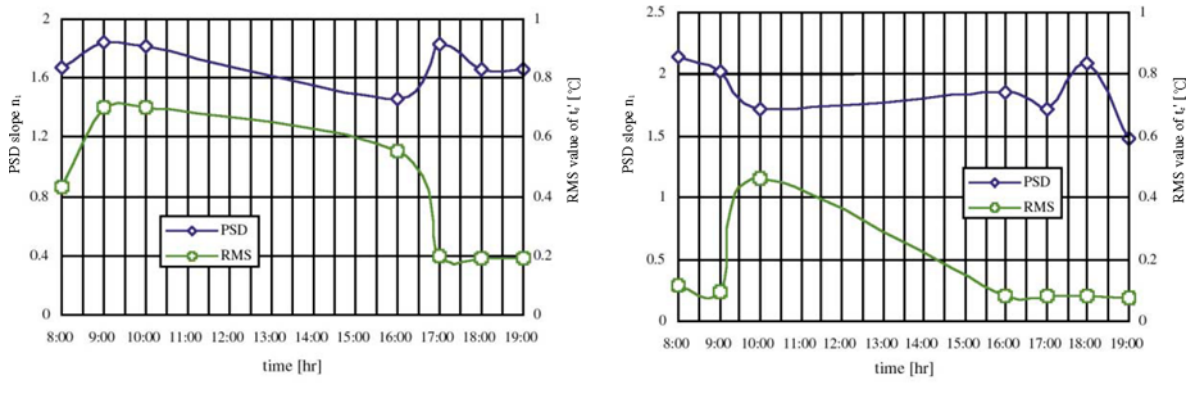

Fig. 11. Comparison of PSD slope n_1 and RMS value between static and dynamic thermal images.

5.2 RMS Values of Variations

The magnifications of environmental factors and objects are defined by the ratio of outdoor to indoor RMS values in Table 1. According to this result, it is explained that the outdoor variation is generally larger than the indoor. The environmental factors are strongly influenced by meteorological conditions. Measured objects are strongly influenced by wind and atmospheric temperature. Generally, the variation of object with large heat capacity is smaller than that with small one.

Table 1. Magnification of indoor and outdoor RMS values.

environmental factors	atmospheric temperature	wind velocity	humidity	irradiance
magnification	14~68	42~104	4~8	0.6~3.6
temperature of objects	soil	concrete		plywood
magnification	10~30	1.4~2.4		6.1~19.4

5.3 Slope of PSD

According to PSD data on variations of environmental factors and objects, PSD slope in any variation has n_1, n_2 and n_3 depending on meteorological conditions, and all variations have always slope n_1, n_2 (= 0), or n_1, n_2, n_3 (= 0) in this experiment. Table 2 shows the comparison of PSD slope n_1 between outdoor and indoor cases. It can be deduced that outdoor PSD slope n_1 is larger than indoor one, and that outdoor PSD slope n_1 is ranged from 0.9 to 3.8 in comparison with the data described in the reference (Agu et al., 1992).

Table 2. PSD slope n_1 between outdoor and indoor conditions.

environmental factors	atmospheric temperature	wind velocity	humidity	irradiance
outdoor	1.0~3.6	0.9~2.4	1.7~3.7	0.9~2.4
indoor	1.7~2.4	1.0~2.1	1.5~2.7	0.5~1.9
temperature of objects	soil	concrete		plywood
outdoor	1.9~3.8	1.3~3.1		1.5~3.7
indoor	1.2~2.8	0.6~3.2		1.3~2.5

5.4 Effect on Detection Limit of Buried Objects in Soil

Detection limit of buried object by means of Infrared Radiometer is defined by the radiation temperature difference on the thermal image between the points of over the buried object and far from it, and the location of buried object is predicted by investigating the detection limit in course of time (Okamoto et al., 1998; Kamoi et al., 2001). The dynamic behavior of detection limits $\Delta T_{c1}'$, $\Delta T_{c2}'$ are shown in Fig. 12 (a), (b). In Fig. 12 (a) $\Delta T_{c1}' \approx 1.0$ and $\Delta T_{c2}' \approx 1.0$ which show different detection limits due to the effect of some environmental factors, but $\Delta T_{c1}'$, $\Delta T_{c2}' \approx 0$ as shown in Fig. 12 (b) due to the effect of weak environmental factors, where $\Delta T_{c1}' = T_c' - \Delta T_{s1}'$, $\Delta T_{c2}' = T_c' - T_{s2}'$ and T_c', T_{s1}', T_{s2}' are the radiation temperatures at the points a, b, c, respectively.

5.5 Visualization of Buried Objects in the Thermal Images

Figure 13 shows the outdoor thermal images of soil surface with four buried objects of which depth are 5, 10, 20, 30 mm at the points b, c, d and e, respectively from 14:00 to 19:00 on November 7, 2000 (fair). In the case of this experiment we could recognize clearly the existence of 4 buried objects except the one of 30 mm depth. This result means that the effect of environmental factors in Fig. 13 is weak in comparison with that of Fig. 6 as

explained by the radiation temperature distributions corresponding to cross cursor lines shown in both thermal images. Therefore it is very important to investigate the environmental factors when we take the thermal image outdoors, and also to evaluate PSD and RMS values, and their relation between environmental factors and objects to be measured.

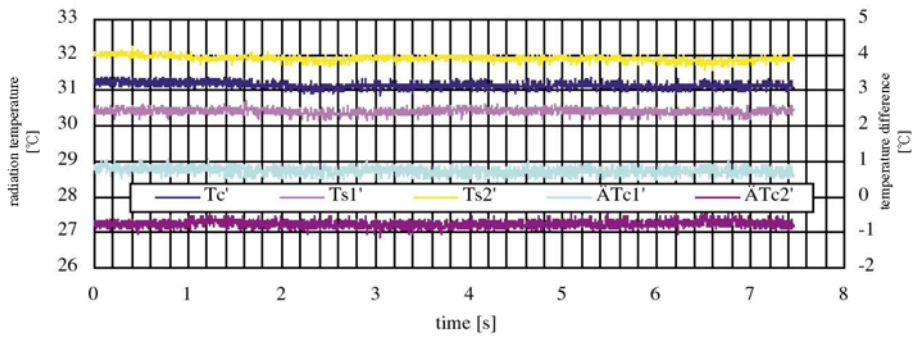

(a) September 27, 2000 (16:00)

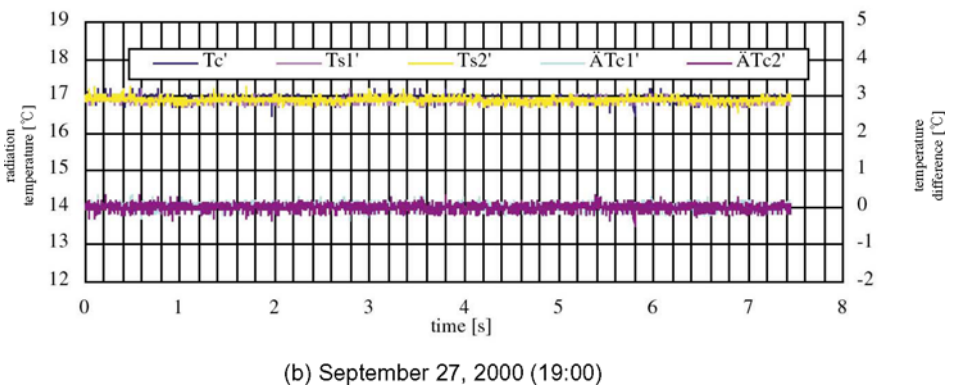

(b) September 27, 2000 (19:00)

Fig. 12. Radiation temperature and its difference of dynamic thermal images on soil surface.

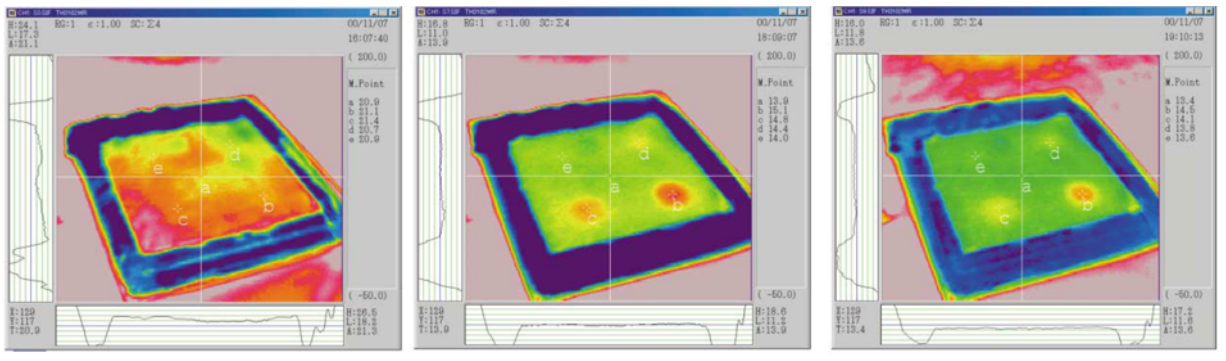

(a) time at 16:00 (before sunset) (b) time at 18:00 (near sunset) (c) time at 19:00 (after sunset)

Fig. 13. Static thermal images with four buried objects.

6. Conclusion

1) The environmental factors are strongly influenced by meteorological conditions, and objects are apt to be influenced by wind and atmospheric temperature. The outdoor variation is generally larger than the indoor one. The variation of object with large heat capacity is smaller than that with small heat capacity.
2) PSD slope in any variation has generally two types of slope of n_1, n_2 (= 0) and n_1, n_2, n_3 (= 0) depending upon meteorological conditions. It can be deduced that outdoor PSD slope n_1 is larger than indoor one, and that outdoor PSD slope n_1 is ranged from 0.9 to 3.8.

3) The variations appeared in thermal images of soil surface with buried object were strongly influenced by the environmental factors that affect the radiation temperature. Therefore the detection limit of the buried object varies in relation to variations of environmental factors.
4) The distribution patterns of RMS and PSD were almost the same outdoors in comparison with the static and dynamic thermal images.
5) It can be predicted that buried metallic object in soil will be visualized corresponding to its depth just before and after the sunset by use of IR camera in case the environmental factors are nearly weak.

References

Agu, M., Teramachi, Y., Yamanaka, K. and Sumiya, M., Some Aspects on Application of Fluctuating Phenomena, Applied Physics, 61-7, (1992), 690.

Hino, M., Spectral Analysis, Asakura Bookstore, (1998), 20.

Kamoi, A. and Okamoto, Y., Experimental Study on the Effect of Environmental Fluctuations Affecting the Thermal Images of Infrared Radiometer, Proc. of SPIE, Vol. 4020, (2000a), 374.

Kamoi , A. and Okamoto, Y., Experimental Study on the Effect of Environmental Fluctuations Affecting the Thermal Images of Soil Surface with Buried Objects by Infrared Radiometer, Proc. of QIRT, Vol. 64, (2000b), 1.

Kamoi, A., Okamoto, Y. and Kondo T., Inspection of Buried Object by Using Infrared Thermography, Inspection Engineering, 6-2, (2001), 9.

Musha, T., 1/*f* Fluctuation Appeared in Living Body, Nature, Vol. 11, (1979), 60.

Okamoto, Y., Kamoi, A. and Ishii, T., Study of Remote Sensing Visible and Infrared Method of Underground Buried Objects Using Thermal Image Technique, Proc. of SPIE, Vol. 3056, (1997), 33.

Okamoto, Y., Kamoi A. and Ishii, T., Thermal Analysis on Internal and Surface Flaws by Means of Infrared Radiometer", Proc. of QIRT, Vol. 60, (1998), 71.

Author Profile

Arao Kamoi: He received his M.Sc. (eng.) in Mechanical Engineering in 1964 from Waseda University. He was a co-researcher of Professor Emeritus H. Tanaka in Department of Jet Propulsion from 1970 to 1972 at Institute of Space and Aeronautical Science of the University of Tokyo, and he was granted his Degree of Dr. in Engineering in 1979 at Aeronautical Engineering Department from the University of Tokyo. Then, he became Professor of Mechanical Engineering Department in 1991 and Professor of Grad. School of Science and Arts in 1992 at the University of East Asia after 25 years' research working at Toyo Kohan Co..

Yoshizo Okamoto: He entered Japan Atomic Energy Research Institute in 1958 and became the head of Department of Japan Materials Testing Reactor (JMTR) in 1980 at Oarai Research Establishment. He received his Degree of Dr. in Engineering in 1973 at Mechanical Engineering Department from the University of Tokyo. He became Professor of Faculty of Engineering in 1982 at Ibaraki University. Then he later became Professor of System Engineering Department at University of East Asia in 1996 and retired in February 2001.